

# **Buoyancy and stability analysis of floating offshore wind turbines**

Ieva Bockute

150013767

School of Science & Engineering

University of Dundee

Honours Project Thesis

Supervisor: Dr Masoud Hayatdavoodi

March 2019

# ABSTRACT

To meet global energy needs and to minimise global warming problem, renewable energy has become a popular way to produce energy. Compared with the other renewable energy sources, wind energy has a relatively high output and therefore is the most attractive option. To avoid visual impacts and get an access to stronger wind fields, floating offshore wind turbines were introduced. However, with floating offshore wind turbines, there comes a problem of how to ensure the buoyancy and stability of such structures. As a result, this thesis will focus on performing the hydrostatic analysis of a chosen offshore wind turbine platform by writing computer codes using the programming language - Fortran.

# CONTENTS

ABSTRACT.....	ii
LIST OF FIGURES .....	v
LIST OF TABLES .....	vi
NOTATIONS.....	vii
CHAPTER ONE – INTRODUCTION .....	1
1.1 Introduction.....	1
1.2 Aims and objectives.....	2
CHAPTER TWO – LITERATURE REVIEW .....	3
2.1 Importance of energy and its consumption.....	3
2.2 Renewable energy.....	4
CHAPTER THREE – WIND POWER.....	5
3.1 Wind power.....	5
3.2 Onshore and Offshore .....	5
3.3 Floating Platforms.....	6
3.3 World’s First Floating Offshore Wind Farm .....	8
CHAPTER FOUR – FLOATING OFFSHORE WIND TURBINE .....	10
4.1 Description.....	10
4.2 Dimensions .....	11
CHAPTER FIVE – HYDROSTATIC ANALYSIS .....	13
5.1 Stability.....	13
5.2 Draft .....	14
5.3 Centre of Gravity .....	16
5.4 Centre of Buoyancy .....	21
5.5 Metacentric radius.....	22
5.6 Metacentric height .....	25
5.7 Righting arm .....	26
CHAPTER SIX – PROGRAMMING .....	28
6.1 Input .....	28
CHAPTER SEVEN – RESULTS .....	29
7.1 Results.....	29
CHAPTER EIGHT – CONCLUSION .....	33
REFERENCES .....	34
APPENDICES .....	37

Appendix A – Input and Instruction files .....	37
Appendix B – Hydrostatic analysis code .....	38
Appendix C – Achieved results .....	42
Appendix D – MATLAB code .....	42
Appendix E – data.txt file, righting arm values (highlighted value- maximum righting arm)	43

# LIST OF FIGURES

Figure 1 Primary energy consumption in 2015 (Source of data: World Energy Council, 2016 ).....	3
Figure 2 Growth of the offshore wind energy capacity from 1990 to 2007 (Esteban et al., 2011) .....	5
Figure 3 Distribution of the offshore wind megawatts in operation in the different countries at the beginning of 2009 (Esteban et al., 2011) .....	6
Figure 4 SPAR, Semi-Submersible and TLP wind turbine systems.....	8
Figure 5 Wind turbine's height compared to other well-known structures (Equinor, n.d.).....	9
Figure 6 Illustration of the turbine moorings and layout (Equinor, n.d.).....	9
Figure 7 The arrangement of the triangular raft (Wong, 2015) .....	10
Figure 8 Positive, Neutral and Negative stability conditions .....	13
Figure 9 Hollow cylinder, the shape of the pontoon and column.....	15
Figure 10 Linear measurements in stability.....	17
Figure 11 Drawing of the triangular platform with the turbines. Front view (Lamei, 2018) ..	18
Figure 12 Reference point with an intersection view of the structure (Lamei, 2018). .....	19
Figure 13 Top view of the structure. Right triangle.....	21
Figure 14 Waterplane areas from plan and side views .....	24
Figure 15 Structure measurements when it heels .....	27
Figure 16 Centre of buoyancy flowchart .....	28
Figure 17 Curve of static stability with a heeling angle varying from 0 to 90 degrees. ....	30
Figure 18 Curve of static stability with heeling angle varying from 0 to 180 degrees.....	31

# LIST OF TABLES

Table 1 Lifetime emissions of carbon dioxide for various power generation technologies (Esteban et al., 2011). .....	4
Table 2 The proposed values for the different properties for the Carlos Wong triangular raft	12
Table 3 Distance from the keel to the object's centre of mass in z, x and y directions .....	20
Table 4 Distance from the keel to submerged structural member's centre of mass in z, x and y directions.....	22
Table 5 The formulas, which are used to find the waterplane areas.....	24
Table 6 Distance $y$ on different axis .....	25
Table 7 Achieved results.....	29

# NOTATIONS

$\overline{BM}$ : metacentric radius

$\overline{GM}$ : metacentric height

$\overline{GZ}$ : righting arm

$\overline{KB}$ : centre of buoyancy

$\overline{KG}$ : centre of gravity

$A_{wp}$ : waterplane area

$F_B$ : buoyant force

$g$ : gravitational acceleration,  $9.81\text{m/s}^2$

$h_{cc}$ : height of the column

$h_t$ : height of the turbine

$I_T$ : moment of inertia of the object about an axis through its centre of mass

$I_T$ : transverse moment of inertia of the waterplane

$K_{g_i}$ : distance from the keel to the structural member's  $i$  centre of mass

$l_p$ : length of pontoon

$m$ : mass of the structure

$m_t$ : mass of the whole wind turbine

$q$ : density

$q_c$ : density of the concrete,  $2400\text{kg/m}^3$

$q_w$ : density of the salted water,  $1025\text{kg/m}^3$

$r$ : radius

$r_{ccin}$ : inner radius of the column

$r_{ccout}$ : outer radius of the column

$r_{pin}$ : inner radius of the pontoon

$r_{pout}$ : outer radius of the pontoon

$V$ : volume

$V_{disp}$ : volume of the displaced fluid

$V_n$ : underwater volume of the submerged structural member  $n$

$W$ : weight of the whole structure

$W_B$ : weight of the ballast

$W_c$ : weight of the column

$w_i$ : weight of the structural member  $i$

$W_p$ : weight of the pontoon

$W_t$ : weight of the turbine

$W_{tot}$ : total weight of the structure

$x_B$ : x axis coordinate of the centre of buoyancy

$x_{bn}$ : distance from the coordinate system to the centre of mass of the submerged structural member  $n$ , on axis x

$y_B$ : y axis coordinate of the centre of buoyancy

$y_{bn}$ : distance from the coordinate system to the centre of mass of the submerged structural member  $n$ , on axis y

$z_B$ : z axis coordinate of the centre of buoyancy

$z_{bn}$ : distance from the coordinate system to the centre of mass of the submerged structural member  $n$ , on axis z

$\pi$ : mathematical constant,  $\pi=3.14$

# CHAPTER ONE – INTRODUCTION

## 1.1 Introduction

Electricity is one of the most important innovations of all time. It has now become a part of our daily lives. We use it not only at home for all our appliances such as light or computers, but for travelling and health, welfare services as well. However, the need for electricity increases every year. It is estimated that the demand of electricity could increase from around 65GW from 2018 up to 75 or 80GW in 2050 (Energy and Climate Intelligence Unit, 2018). This will result in increased emissions of various greenhouse gasses into our atmosphere. These emissions are responsible for the increasing earth's average temperature, which could rise up to 1-3.5°C by the end of twenty-first century (Sen, 2018). What is more, the fossil fuel reservoirs are rapidly decreasing and as a result the distinction of such reservoirs is a possible risk (Sen, 2018). Therefore, it is necessary to minimise the risk of running out of fossil fuels and making the global warming situation worse. As a result, humans came up with an idea to use renewable technology to make electricity.

Renewable technologies use natural fuel sources to produce electricity. The criteria for natural fuel source is for it to be naturally replenishing. Although renewable energy has a lot of advantages such as not being that toxic for the environment, requiring less maintenance or being able to replenish itself, it has its disadvantages as well. The disadvantages include the higher price, its performance dependence on weather conditions and danger to animals, e.g. wind turbines can kill birds (Iglesia et al., 2017).

During the first quarter of 2018, 30.1 percent of all electricity generated in the United Kingdom was generated by renewables (Department for Business, Energy & Industrial Strategy, 2018). Although this percentage is already higher than the percentage of 2017's first quarter by 3.1 percent (Department for Business, Energy & Industrial Strategy, 2018), it still has a lot of space for development and improvement.

There are many different renewable energy sources such as waves, sun, water and wind. This thesis will focus on the lateral one. Wind energy has spread the most due to the relatively high output and the little disruption of ecosystems (Energy4me.org., 2018). This type of energy also can be split into two categories: the onshore and offshore one. Due to the access to stronger wind fields and therefore higher energy output, the offshore wind energy is becoming more popular compared to the onshore one. It also has a smaller impact on the environment (Esteban

et al., 2011). Offshore wind turbine is more durable than the onshore one and can be used for up to 30 years and generate 50 percent more energy (Adepipe, Abolarin and Mamman, 2018).

However, with offshore wind turbines there comes a lot of new challenges and one of them is how to install a floating offshore wind turbine and make sure it is stable and floating. To find an answer to this question the hydrostatic analysis of a particular wind turbine should be done. Therefore, this thesis will focus on hydrostatic analysis and with the help of programming language Fortran, a code for hydrostatic calculations will be prepared. The achieved results will be discussed as well.

## 1.2 Aims and objectives

The aim of this project is to perform the buoyancy and stability analysis of floating offshore wind turbine with the help of in-house computer codes.

To achieve this aim, the following objectives were set:

- Determine stability and its requirements for floating offshore wind turbine.
- Determine the centre of buoyancy, centre of gravity, metacentric height and righting arm etc.
- Damage stability analysis for light and various ballast conditions.
- Intact stability analysis for light and various ballast conditions.
- Carry out stability analysis using a programming language – Fortran.

## CHAPTER TWO – LITERATURE REVIEW

### 2.1 Importance of energy and its consumption

Electricity is one of the most important innovations of all time. As stated previously, it has now become a part of our daily lives. To receive electricity, it first needs to be generated (convert a form of energy into electricity). As a result, materials such as coal, nuclear power, natural gases and other natural resources are used as primary energy sources. Although, the wind and solar capacity for power generation globally increased by 200GW between 2013 and 2015 (World Energy Council, 2016), the most popular type of primary energy consumption in 2015 was oil, coal and gas (World Energy Council, 2016). Together with nuclear energy, in 2015 non-renewable energy sources reached 90.43% of all energy consumed. The primary energy consumption in 2015 can be seen in Figure 1.

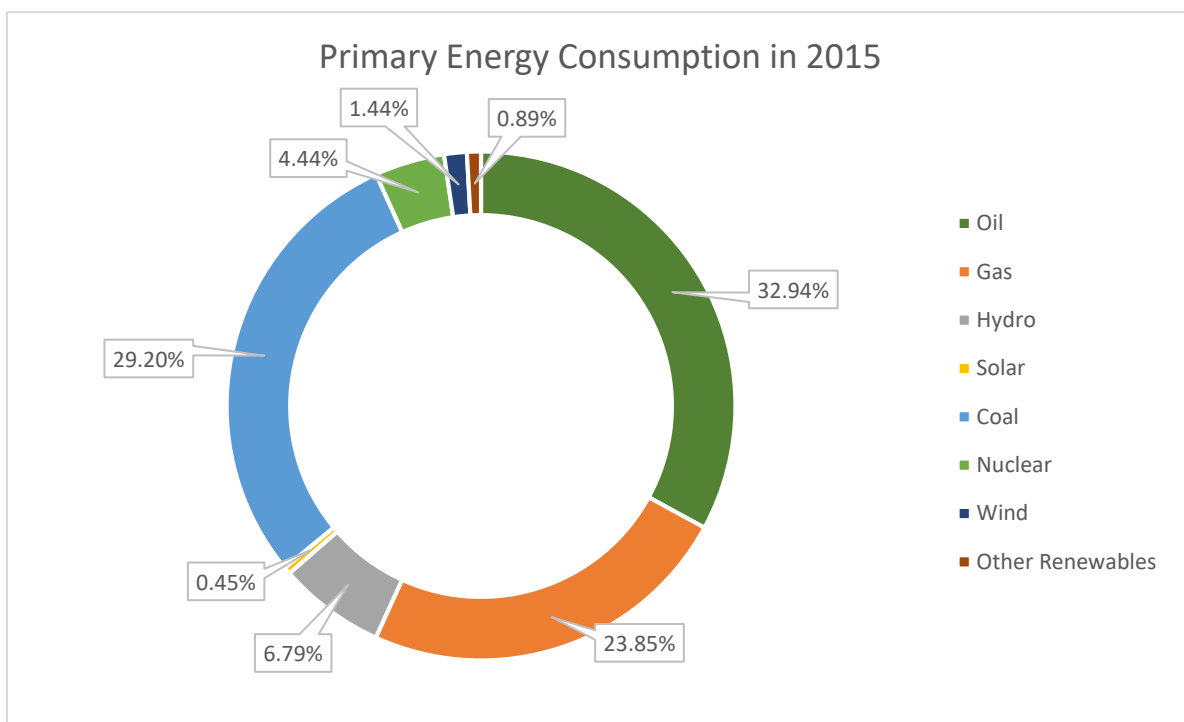


Figure 1 Primary energy consumption in 2015 (Source of data: World Energy Council, 2016 ).

Although, it seems as the most popular choice of generating electricity, non-renewable energy sources have one main disadvantage: they release pollutant particles into the air, water and land. These particles are known as greenhouse gasses, which are responsible for the global warming situation. The amount of how much carbon dioxide each source of energy emitted in 2011 can be seen in Table 1.

	<b>Carbon Dioxide Emissions (t/GWh)</b>
Coal	964
Oil	726
Gas	484
Nuclear	8
Wind	7
Photovoltaic	5
Large Hydro	4

*Table 1 Lifetime emissions of carbon dioxide for various power generation technologies (Esteban et al., 2011).*

Nuclear energy does not emit greenhouse gases, but it produces a radioactive waste, which is extremely toxic and increases the risk of cancer, blood diseases etc. (Morse, 2013). A great example of the damages that radioactive waste can do is the Chernobyl disaster which occurred in 1986 on April 26, in Ukraine. Within a few weeks of the disaster more than 28 people were dead (McCall, 2016), while the soil, trees and water bodies were contaminated and made the territory not possible to live in (International Atomic Energy Agency, 2001).

The other disadvantage of non-renewable energy is that fossil fuel reserves are finite. Therefore, if the rate at which the world consumes them will not decrease, the reserves of fossil fuels will start to run out. As the demand of energy increases each year, to avoid running out of fossil fuels and to improve the climate change situation, humans came up with an alternative way of producing energy. The renewable energy was introduced.

## 2.2 Renewable energy

The renewable energy is generated from natural resources that continuously replenish. There are many various renewable energy sources such as solar, wave and wind energy. Technologies used to generate renewable energy are capital intensive and require more expenses to be constructed than the non-renewable ones. On the other hand, renewable energy technologies have lower operational costs (Esteban et al., 2011).

In 2001 renewable energy sources supplied somewhere between 15 and 20 percent of world's total energy demand (Herzog et al., 2001). However, only 2007 was the time when it achieved its 1<sup>st</sup> percent of the electricity generated in the whole world (Esteban et al., 2011).

# CHAPTER THREE – WIND POWER

## 3.1 Wind power

From all the renewable energy sources (excluding hydropower because of its different origin and way of development), the wind energy is spread the widest due to the relatively high output and the little disruption of ecosystems. Estimations suggest that global wind energy would be able to generate between 20,000 TWh and 50,000 TWh of electricity each year. To put this into perspective, the annual global electricity consumption in 2004 was around 17,000 TWh (Esteban et al., 2011). As a result, wind energy alone could generate enough electricity to satisfy the needs of it. Therefore, knowing all the advantages of renewable energy against non-renewable one it is very important that future development takes place. In the future, all the energy could be produced by renewable energy without the danger of fossil fuels going extinct or increasing the temperature of the Earth.

## 3.2 Onshore and Offshore

Wind renewable energy can be split into two categories: onshore and offshore. Smaller impact on the environment and access to stronger wind fields made the offshore wind turbines more popular. Offshore wind turbines also release less noise and saves up the limited land space. The first offshore wind turbine was set in 1990 in Sweden (Esteban et al., 2011). The growth of the offshore wind energy capacity from 1990 up to 2007 can be seen in Figure 2.

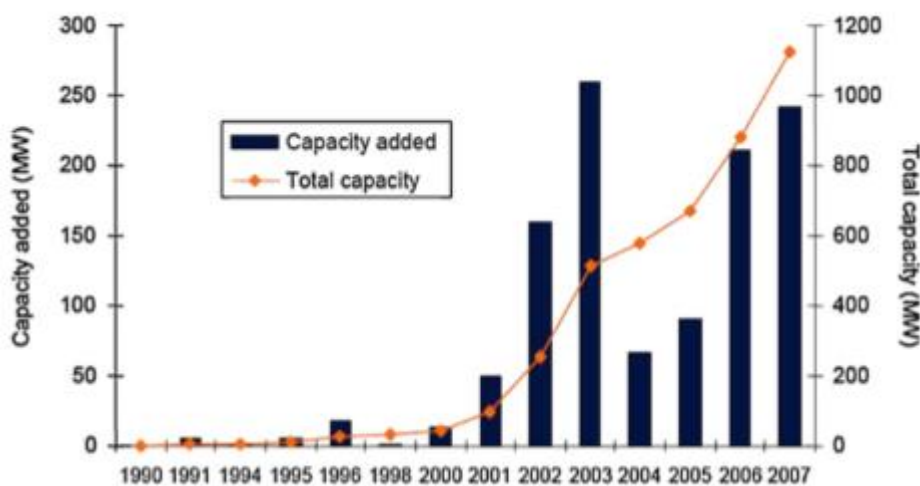


Figure 2 Growth of the offshore wind energy capacity from 1990 to 2007 (Esteban et al., 2011)

As the turbines can be built offshore, where there is more free area than on land, it opens a possibility to build larger wind farms, which also do not leave big visual impact. However, as not all countries have access to the sea or the ocean, it reduces the number of countries which can be at the top of its development. The distribution of the offshore wind power among the different countries can be seen in Figure 3.

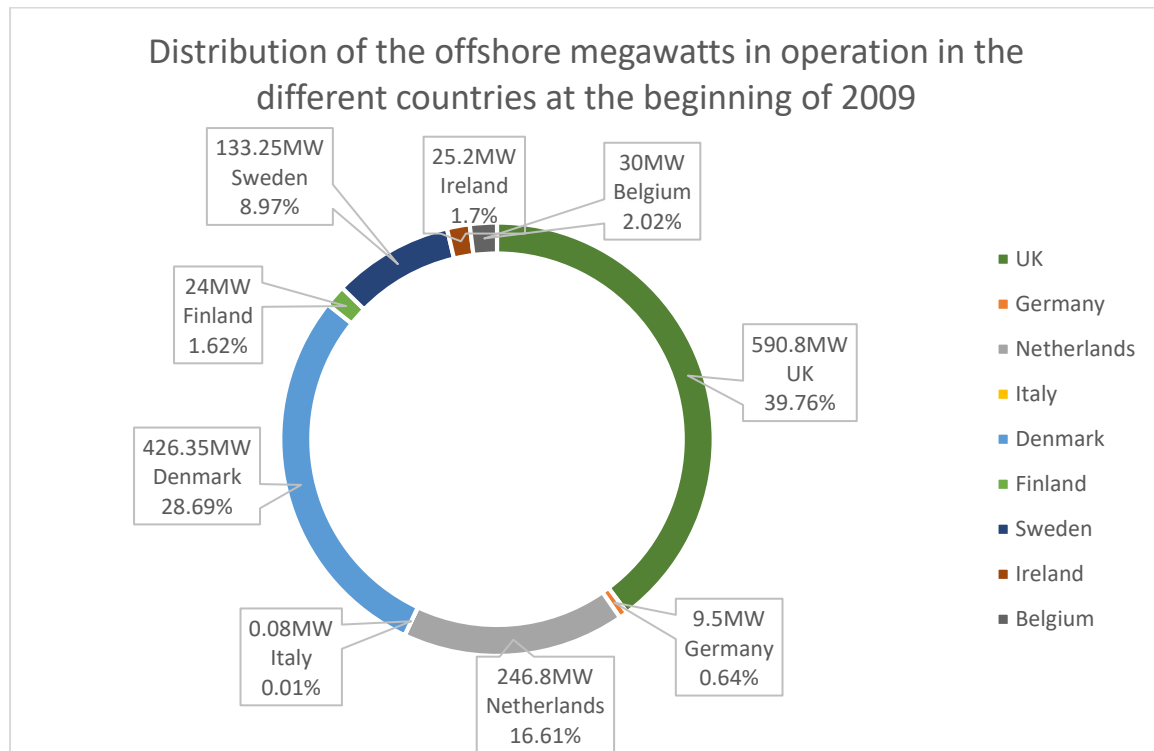


Figure 3 Distribution of the offshore wind megawatts in operation in the different countries at the beginning of 2009 (Esteban et al., 2011)

However, with offshore wind turbines there comes a lot of new challenges. One of them is how to reduce the cost of the construction and operation phases. Because of the high costs of the sea operations, the installation of wind generator turbines offshore is around 33% of the whole project expenses, while the cost of installation onshore reaches 75% of the whole project expenses (Esteban et al., 2011). The other challenge is how to avoid the structure being damaged by the extreme weather conditions, installing and designing an offshore wind turbine which would be floating and stable.

### 3.3 Floating Platforms

The offshore wind turbines can be either fixed foundation or floating. The advantage of floating offshore wind turbines is that they can be installed in deeper waters than the fixed foundation turbines, where they also have access to stronger wind speeds.

There are three main types of floating platforms for the deep water: spar, semi-submersible and tension leg platform. All of them can be seen in Figure 4. In 2011, in the world there were more than 120 semi-submersible, 25 tension leg and 17 spar platforms (Li et al., 2011).

The spar platform is known as the most suitable type of platform for deep water operations. The reason behind this, is that this type of platform has a favourable motion performance, is adaptable to deep water and has joint availability of dry and wet tree drilling (Li et al., 2011). A great example of what depth spar type platform can achieve is the world's deepest offshore oil drilling and production Perdido spar platform located in the waters of Gulf of Mexico. It reaches a water depth of 2380 metres (Li et al., 2011). However, the disadvantage of spar platforms is their huge dimensions, transportation and the installation process. These factors not only increase the cost of the project but generate an extra risk as well.

Another type of offshore floating platform is tension leg platform also known as TLP. This type of platform is quite sensitive to the water depth. The deeper it goes into the water, the more complex gets the design and the construction of the seabed foundation. This as well can affect the safety of the structure. Although, there are TLP that has reached the water depth of 1425 metres (Li et al., 2011).

Semi-submersible platforms consist of large volume pontoons, which are fully submerged into the water and have vertical columns which are submerged as well, however not fully. The production and installation of such type of platform can be relatively cheap compared with TLP and spar platforms. (Li et al., 2011). However, semi-submersible platforms are not that resistant to harsh weather conditions, for example typhoons or hurricanes.

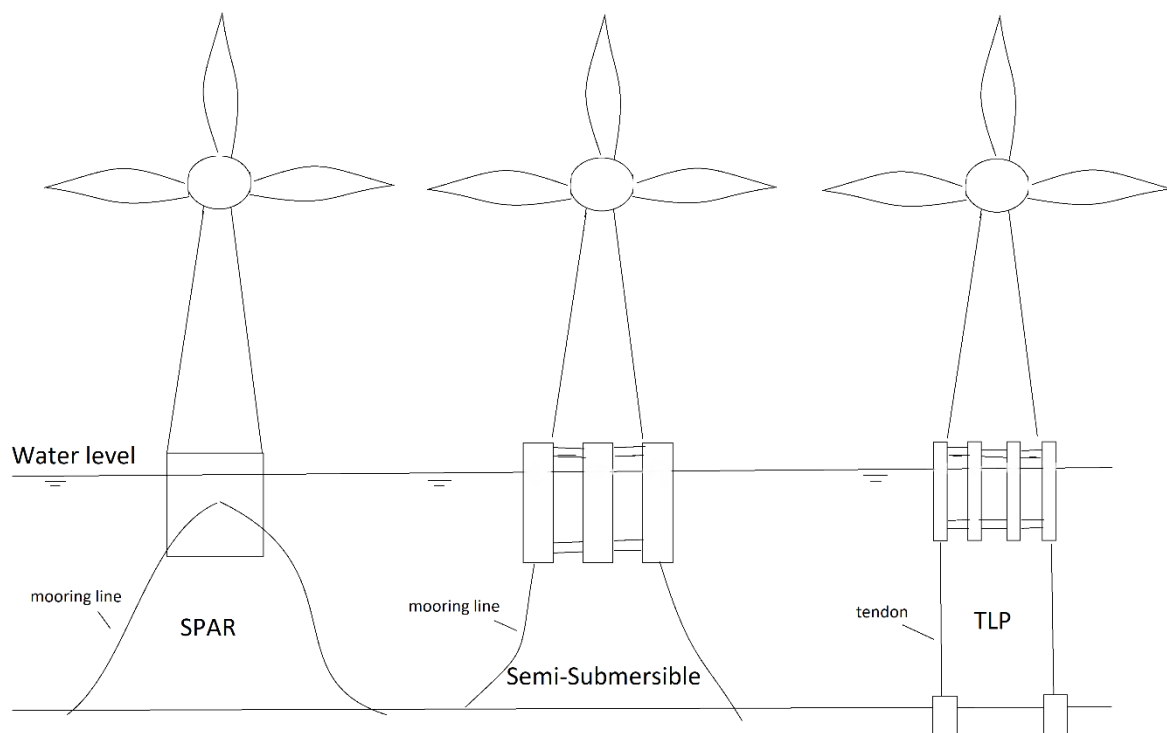


Figure 4 SPAR, Semi-Submersible and TLP wind turbine systems

### 3.3 World's First Floating Offshore Wind Farm

The very first world's floating offshore wind farm also known as Hywind Pilot Park was built in Scotland, around 25km from Peterhead in Aberdeenshire. It was built in 2017 by Equinor (Statoil) and has 5 floating turbines with a total capacity of 30MW. It was estimated that this farm will power around 20,000 households. The whole farm takes up around 4km<sup>2</sup> area in the North Sea with the depth varying from 95m to 120m and the average wind speed in this location being 10m/s. Hywind turbines could be used for water depths up to 800m, while fixed foundation turbines are usually limited for maximum up to 50m depth. The height of each Hywind turbine reaches 258m, the diameter of the rotor is 154m and the height of the hub varies between 82m and 101m (Statoil, 2015). The comparison between the height of Hywind turbine and other famous objects in the world, such as Big Ben in London, can be seen in Figure 5.

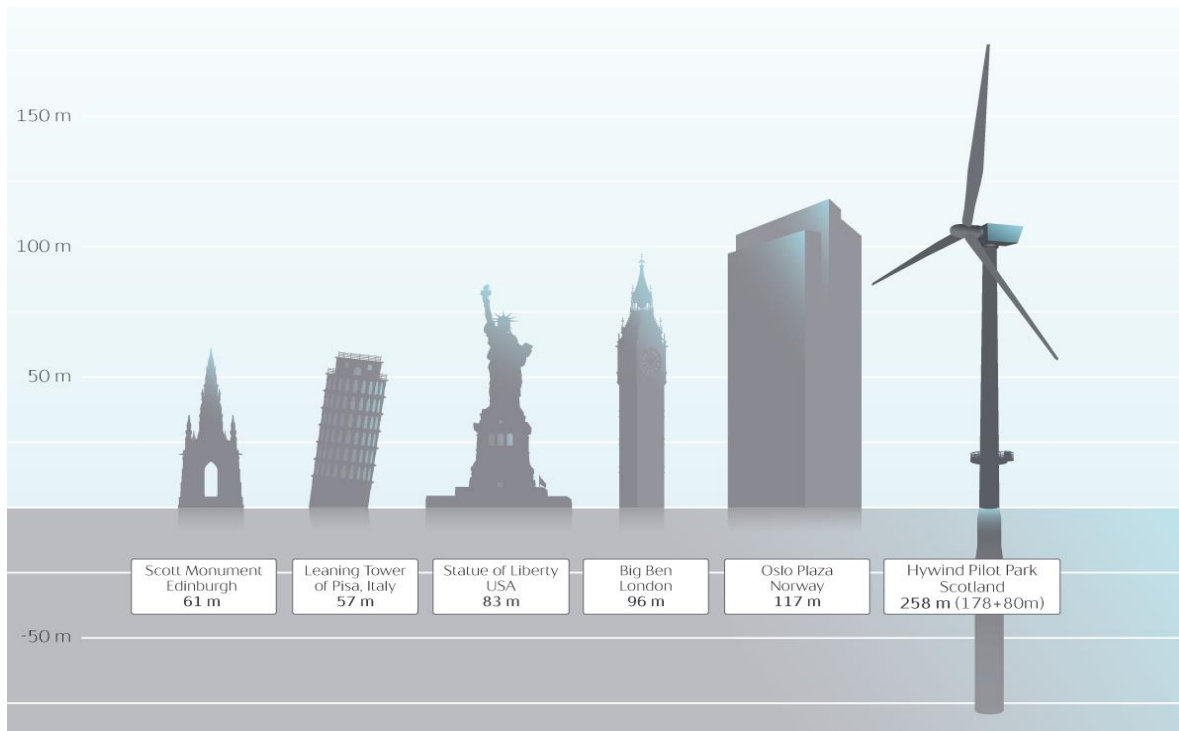


Figure 5 Wind turbine's height compared to other well-known structures (Equinor, n.d.)

To ensure the structure is stable and will not be flipping over, the turbines were attached to the seabed by a three-point mooring spread and anchoring system. The distance between the turbines varied between 720 to 1600m and each of the turbines required three anchors attached to it. While, the radius of the mooring system extended up to 1200m out of each of the turbines (Statoil, 2015). The visualisation of such structure and how it looks under water can be seen in Figure 6.

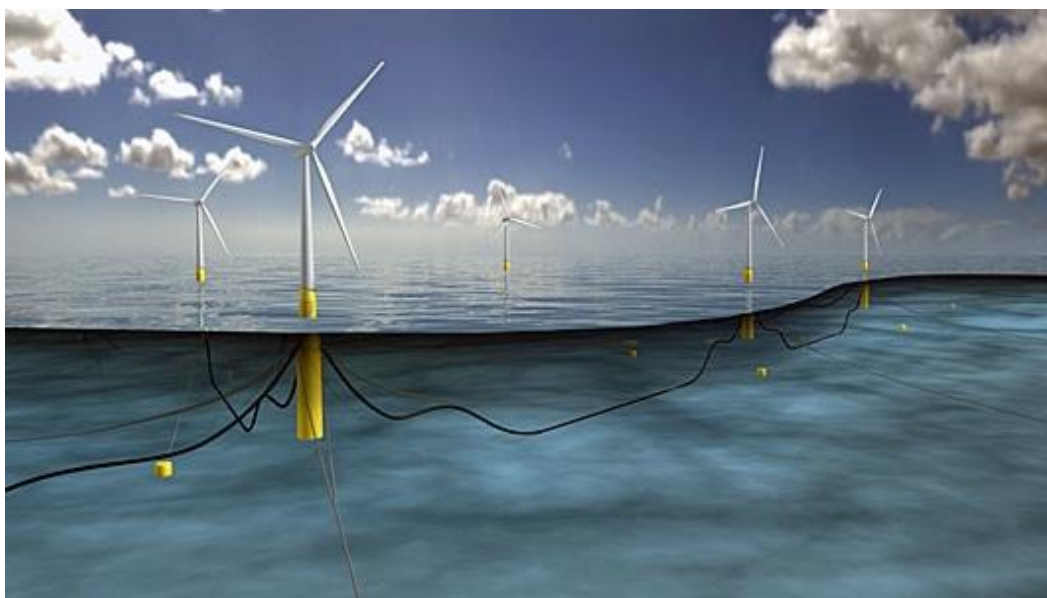


Figure 6 Illustration of the turbine moorings and layout (Equinor, n.d.)

# CHAPTER FOUR – FLOATING OFFSHORE WIND TURBINE

## 4.1 Description

During this project to carry out a hydrostatic analysis, a semi-submersible platform has been chosen. To be more precise, Carlos Wong semi-submerged triangular raft for offshore wind turbine will be used.

This triangular shape raft, supporting three 5MW turbines, is able orientate to wind facing side by itself, while using an eccentric rotation centre.

This turbine consists of three columns, which supports three turbines and three raft beams also known as the pontoons. Distance between the columns are  $2.2 D$ , where  $D$  is the diameter of the turbine rotor (Wong, 2015). As the shape of the raft is triangular, there are two rows of turbines: two turbines in the first row and one in the back row, which is located between the two front turbines. How it looks like can be seen in Figure 7. Such arrangement allows it not to lose any power as the wind reaches the front turbines at the same speed as the rear turbine.



*Figure 7 The arrangement of the triangular raft (Wong, 2015)*

The turning mechanism of this platform is provided by the cable lines and the mooring rope. They also form a single tensioned leg platform that can increase the stability of the platform.

The other thing that provides the stability to the platform are the floaters, also known as columns. They have a hollow cylindrical shape and provide buoyancy to the platform. Also, the way floaters connect to the pontoons, allows for the pontoons together with the wind turbines to float in the water and create a large footprint and a small waterplane area, which make the raft very stable (Wong, 2015).

There is also a ballast, which is used to provide stability for the whole structure. In this case, the ballast holds the water and is located inside the pontoons. It allows for water to move inside and outside of the structure with the purpose to neutralize the effect of the weight which is above the water level (Spon et al., 1874).

To make sure the platform does not float away, a mooring rope is used to provide the node to an anchor, which is placed in the seabed. The anchor is visible in Figure 7.

This structure uses prestressed concrete hollow sections for raft beams and cylindrical floaters. The advantages of using prestressed concrete as the main material rather than steel, includes longer working life and less expenses. This is the result of the concrete being less expensive than steel and fatigue insensitive, which is very important knowing that the structure will be submerged in the water all the time. Also, the structure made of concrete can be casted and joined on the shore of a harbour or even in the harbour if bridge building technique is used, which saves the time and expenses putting the structure together. Thus, concrete material can last up to 100 years without any major maintenance. What is more, the concrete is heavier than steel, therefore the raft beams can be submerged into the depth greater than 14 metres, where it can avoid the actions of the waves and it can be ballasted to balance the buoyancy in order to achieve the suspension state (Wong, 2015).

## 4.2 Dimensions

The values used for this platform to run the calculations are as follows:

<b>Property</b>	<b>Value</b>
Mass of the turbine	697.46 ton
Height of the turbine	177.6 metres
Outer radius of the tower	3 metres
Outer radius of the column	7 metres
Inner radius of the column	6.6 metres
Height of the column	38 metres
Outer radius of the pontoon	4 metres
Inner radius of the pontoon	3.65 metres
Length of the pontoon	264 metres
The density of the water	1025 kg/m <sup>3</sup>
The density of the concrete	2400 kg/m <sup>3</sup>
Ballast volume of the voids	70%

*Table 2 The proposed values for the different properties for the Carlos Wong triangular raft*

# CHAPTER FIVE – HYDROSTATIC ANALYSIS

## 5.1 Stability

The stability is the ability to withstand heeling moments and return the structure to its initial upright position. Heeling moment is usually created by the forces from the wind, waves or currents. To ensure that the structure is stable the buoyancy and stability analysis must be done. First, it must be determined whether the structure is moving and is hydrodynamic or whether it is not in motion and therefore is in hydrostatic equilibrium.

There are three different stability conditions:

- **Positive Stability** – It is achieved when the metacentre is located above the structure's centre of gravity. Also, when the structure is in positive stability and it leans, the righting arm appears and tries to return the structure to its initial position.
- **Neutral Stability** – achieved when the metacentre and the centre of gravity of the structure is at the same location. If the structure leans, no righting arm appears to bring it back to its vertical position. It is the most unwanted situation for the structure.
- **Negative Stability** – this time the centre of gravity is located above the metacentre. In case the structure leans, negative righting arm appears, which will make the structure roll over (Surface Officer Warfare School, n.d.).

Different stability conditions can be seen in Figure 8.

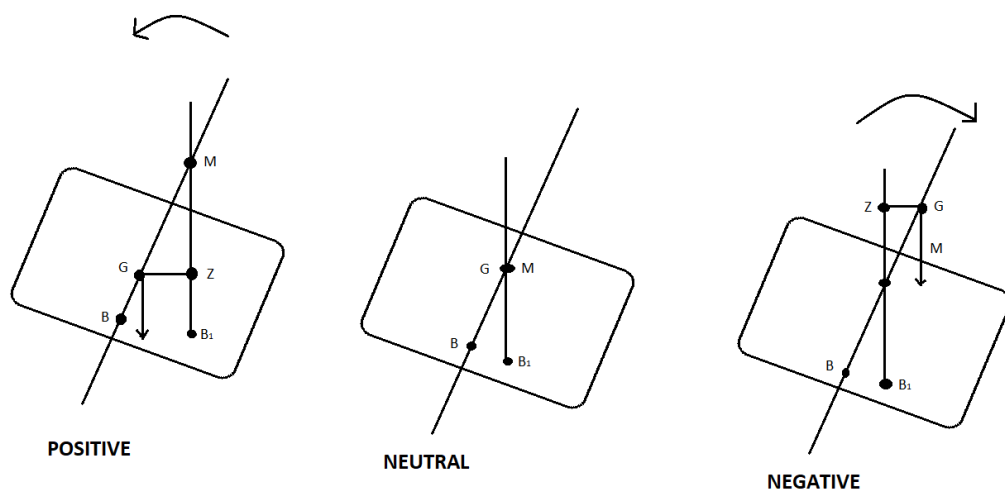


Figure 8 Positive, Neutral and Negative stability conditions

This time the floating offshore wind turbine is assumed to be in hydrostatic equilibrium. Therefore, to check platform's stability the following values should be computed: weight of the structure, draft, centre of gravity, centre of buoyancy, metacentric radius, metacentric height, righting moment and righting arm.

## 5.2 Draft

The vertical distance between the bottom of the keel and the waterline is called draft (T). The value of the draft increases with the additional weight of the structure. Archimedes' principle states that the body submerged in a fluid, liquid or gas at rest has an upward force also known as buoyant force and this force's magnitude is equal to the weight of the fluid displaced by the body. This put into equation looks like this:

$$F_B = W \quad (1)$$

Where,  $F_B$  – the buoyant force and  $W$  – is the weight of the whole structure.

To find the weight of the whole structure its material properties such as the density of it and dimensions, its length, radius, diameter and height, should be known.

The formula for the weight is:

$$W = m * g \quad (2)$$

Where,  $m$  - mass of the structure and is equal to volume times density of the structure's material, whereas volume depends on the shape of the object,  $g$  - acceleration of gravity and is equal to  $9.81 \text{ m/s}^2$ .

The structure used for computations, Carlos Wong platform, has 9 main structural members: 3 pontoons, 3 columns and 3 turbines.

The weight of the pontoon can be found using this formula:

$$W_p = \pi * (r_{pout}^2 - r_{pin}^2) * l_p * q_c * g \quad (3)$$

Where,  $r_{pout}$  and  $r_{pin}$  – outer and inner radius of the pontoon,  $q_c$  – density of the concrete,  $l_p$  - length of pontoon and  $g$  - is the gravitational acceleration, which is equal to  $9.81 \text{ m/s}^2$ .

The formula to find the weight of the pontoon and the column is the same as both structural members have the same type of shape – hollow cylinder.

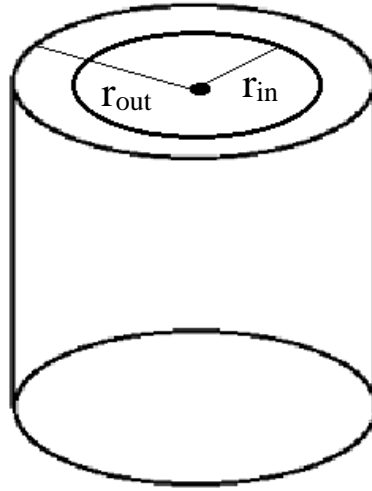


Figure 9 Hollow cylinder, the shape of the pontoon and column

Although, as their dimensions are different, the formula rearranged for the weight of the column is as follows:

$$W_{cc} = \pi * (r_{ccout}^2 - r_{ccin}^2) * h_{cc} * q_c * g \quad (4)$$

Where,  $r_{ccout}$  and  $r_{ccin}$  – outer and inner radius of the column,  $h_{cc}$  – the height of the column.

As mentioned before, the mass of the turbine is given, therefore the formula of the turbine's weight can be simplified to:

$$W_t = m_t * g \quad (5)$$

Where,  $m_t$  – is the mass of the turbine (which includes the nacelle, motor and tower).

There is also a ballast, which adds extra weight to the structure. The ballast in this case is located inside the pontoon, therefore to find the weight of it, the inner radius of the pontoon will be used for its weight calculations.

$$W_B = \pi * r_{pin}^2 * l_p * q_f * g \quad (6)$$

It is also assumed that there is 70% ballast volume of the voids. As a result, only 70% of the previously calculated weight of the ballast value should be used. Hence, the value is multiplied by 0.7.

As the total weight of the whole structure includes the sum of all the structural members plus the ballast, the formula is as follows:

$$W_{total} = 3 * (W_p + W_{cc} + W_t) + 0.7 * W_B \quad (7)$$

The buoyant force is equal to:

$$F_B = q_f * V_{disp} * g \quad (8)$$

Where,  $q_f$  – the density of fluid the structure is submerged in,  $V_{disp}$  – volume of the fluid displaced.

Inserting Equation 8 into the Equation 1, gives:

$$V_{disp} = \frac{W}{q_f g} \quad (9)$$

Using this equation, the volume of the fluid displaced is found. The value of it can be used to find the draft. It is important to state that it is assumed that the pontoons in this case are fully submerged and the turbines are above the water. Taking this into consideration, the formula to find the draft can be written as:

$$V_{disp} = 3 * \left( (\pi * (r_{ccout}^2 - r_{ccin}^2) * Draft) + (\pi * (r_{pout}^2 - r_{pin}^2) * l_p) \right) \quad (10)$$

And the draft is equal to:

$$Draft = \frac{\frac{V_{disp}}{3} - (\pi * r_{pout}^2 * l_p)}{\pi * r_{ccout}^2} \quad (11)$$

The code written for this computation can be seen in the Appendix B.

### 5.3 Centre of Gravity

The point where it is assumed that the entire weight of the structure acts, is called the centre of gravity. The centre of mass and centre of gravity are in the exact same position. It is a fixed point and does not move if there is no additional weight added. The centre of gravity can be seen in Figure 10 as G.

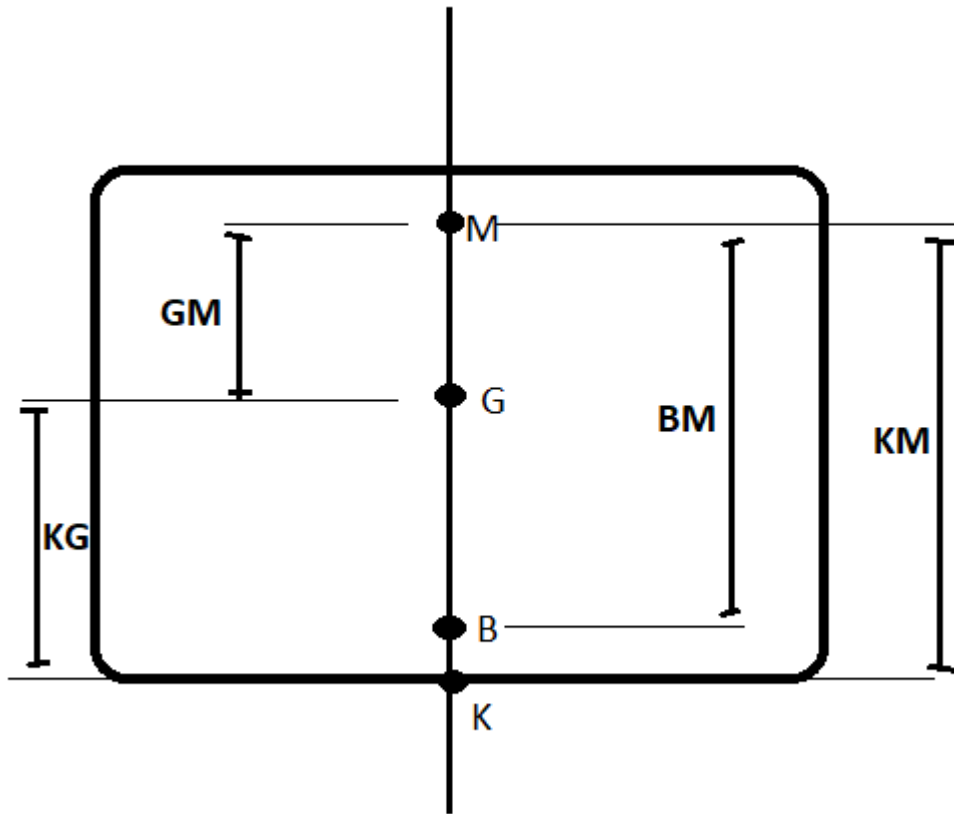


Figure 10 Linear measurements in stability

To find the centre of gravity of the whole structure, where there are a few structural members, the following formula is used:

$$\overline{KG} = \frac{\sum w_i \overline{Kg}_i}{\sum w_i} \quad (12)$$

Where,  $\overline{KG}$  – is the centre of gravity,  $w_i$  - is the weight of the structural member  $i$ ,  $Kg_i$ - is the distance from the keel to the structural member's  $i$  centre of mass.

In this case, the structure is triangular shape, therefore the calculation process involves the summation of the moments of the weights of all the particles that make up this platform (Lotha, 2018).

As noted before, there are 9 structural members: 3 pontoons, 3 columns and 3 turbines and a ballast. All of the structural members can be seen in Figure 11.

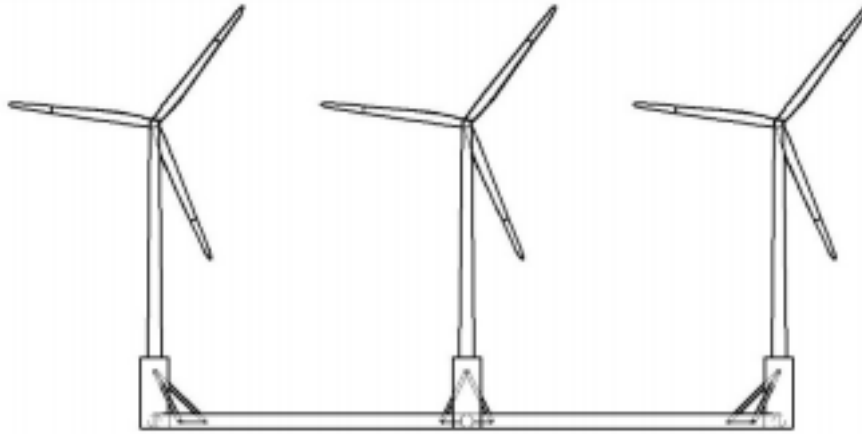


Figure 11 Drawing of the triangular platform with the turbines. Front view (Lamei, 2018)

As a result, the Equation 12 is rearranged:

$$\overline{KG} = \frac{w_1 * \overline{Kg_1} + w_2 * \overline{Kg_2} + \dots + w_9 * \overline{Kg_9}}{W_{total}} \quad (13)$$

This formula can be used to find the location of the centre of gravity with finding its coordinates on different axes z, x and y. Where, z axis is the vertical axis that points upwards, x is the longitudinal axis that points ahead, and y is the transverse axis.

The reference point, which was used not only for finding the centre of gravity, but for finding the other values as well can be seen in Figure 12. It is located at the left bottom of the structure.

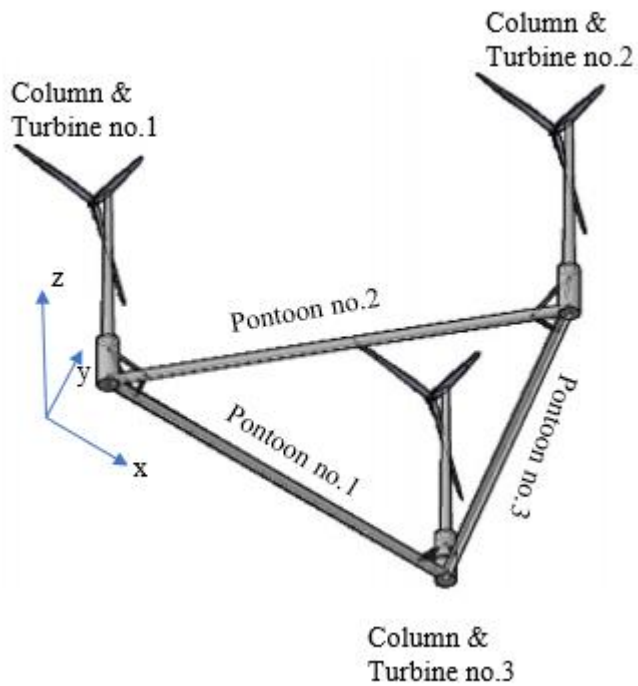


Figure 12 Reference point with an intersection view of the structure (Lamei, 2018).

While using Equation 13, it is important to remember that the weight of the structural member always stays the same, despite the axis you are looking at. However, the thing that changes with different axes is the distance from the keel to the structural member's centre of mass. The values used for  $Kg_i$  for each of the structural members on different axis, where the reference point is the one seen in Figure 12, are given in Table 3.

	Distance from the keel to object's centre of mass in z direction	Distance from the keel to object's centre of mass in x direction	Distance from the keel to object's centre of mass in y direction
<b>Pontoon no.1</b>	$r_{pout}$	$\frac{l_p}{2}$	$r_{pout}$
<b>Pontoon no.2</b>	$r_{pout}$	$\frac{l_p}{4}$	$\frac{\sqrt{3} * l_p}{4}$
<b>Pontoon no.3</b>	$r_{pout}$	$\frac{3 * l_p}{4}$	$\frac{\sqrt{3} * l_p}{4}$
<b>Column no.1</b>	$\frac{h_{cc}}{2}$	$r_{ccout}$	$r_{ccout}$
<b>Column no.2</b>	$\frac{h_{cc}}{2}$	$\frac{l_p}{2}$	$\frac{\sqrt{3} * l_p}{2}$
<b>Column no.3</b>	$\frac{h_{cc}}{2}$	$l_p$	$r_{ccout}$
<b>Turbine no.1</b>	$h_{cc} + \frac{h_t}{2}$	Outer radius of the turbine's tower	Outer radius of the turbine's tower
<b>Turbine no.2</b>	$h_{cc} + \frac{h_t}{2}$	$\frac{l_p}{2}$	$\frac{\sqrt{3} * l_p}{2}$
<b>Turbine no.3</b>	$h_{cc} + \frac{h_t}{2}$	$l_p$	Outer radius of the turbine's tower

Table 3 Distance from the keel to the object's centre of mass in z, x and y directions

These values were achieved from the geometry calculations. As the platform is triangular shape, the distance from the reference point to the pontoon no.2 in y direction in the Figure 13 can be seen as the distance X. As ABC makes the right triangle, the AB is equal to half the length of AC. AC in this case is equal to  $l_p/2$  and therefore AB is equal to half of it:  $l_p/4$ .

Then using the Pythagorean theorem, the length of CB or X is found using the Equation 14.

$$X = \sqrt{\left(\frac{l_p}{2}\right)^2 - \left(\frac{l_p}{4}\right)^2} = \frac{\sqrt{3} * l_p}{4} \quad (14)$$

Using the same geometry rules the other distances are found as well.

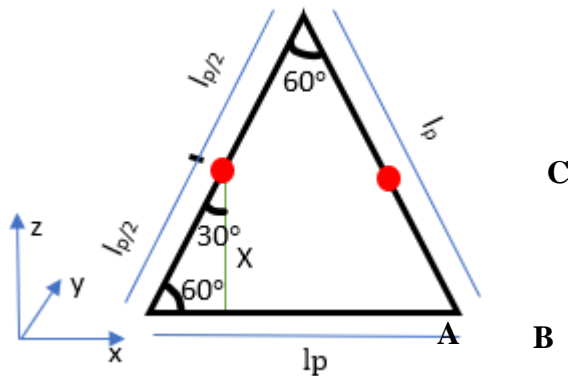


Figure 13 Top view of the structure. Right triangle

The written code to find the coordinates of centre of gravity can be seen in Appendix B.

## 5.4 Centre of Buoyancy

The centre of mass for the volume of the fluid displaced is called – centre of buoyancy (Parsons, n.d.).

Different to the centre of gravity, centre of buoyancy is not a fixed point and moves depending on whether the structure gets heavier or moves in any way (e.g. heels). For example, if the distance between the centre of buoyancy and the centre of gravity is increasing, the rocking of the structure is increasing as well (Parsons, n.d.). Therefore, it is important to know where the centre of buoyancy is located, in order to ensure the stability of the structure.

To find the location of the centre of buoyancy on axes z, x and y, the following formulas are used:

$$z_B = \frac{1}{V_{disp}} \sum_{n=1}^N z_{bn} * V_n , \quad x_B = \frac{1}{V_{disp}} \sum_{n=1}^N x_{bn} * V_n , \quad y_B = \frac{1}{V_{disp}} \sum_{n=1}^N y_{bn} * V_n \quad (15)$$

Where,  $V_{disp}$  – volume of the fluid displaced,  $z_{bn}$ ,  $x_{bn}$ ,  $y_{bn}$  – distance from the reference point to the centre of mass of the submerged structural member  $n$ , for different axes,  $V_n$  –underwater volume of the submerged structural member  $n$ .

The distances between the reference point and the centre of mass of the submerged structural member  $n$  will be different, depending from which axis it is viewed. Assuming only the pontoons and columns are submerged into the water, the distances can be seen in Table 4.

	<b>Distance from the keel to submerged structural member's centre of mass in z direction</b>	<b>Distance from the keel to submerged structural member's centre of mass in x direction</b>	<b>Distance from the keel to submerged structural member's centre of mass in y direction</b>
<b>Pontoon no.1</b>	$\Gamma_{pout}$	$\frac{l_p}{2}$	$\Gamma_{pout}$
<b>Pontoon no.2</b>	$\Gamma_{pout}$	$\frac{l_p}{4}$	$\frac{\sqrt{3} * l_p}{4}$
<b>Pontoon no.3</b>	$\Gamma_{pout}$	$\frac{3 * l_p}{4}$	$\frac{\sqrt{3} * l_p}{4}$
<b>Column no.1</b>	$\frac{Draft}{2}$	$\Gamma_{ccout}$	$\Gamma_{ccout}$
<b>Column no.2</b>	$\frac{Draft}{2}$	$\frac{l_p}{2}$	$\frac{\sqrt{3} * l_p}{2}$
<b>Column no.3</b>	$\frac{Draft}{2}$	$l_p$	$\Gamma_{ccout}$

Table 4 Distance from the keel to submerged structural member's centre of mass in z, x and y directions

After the  $z_B$ ,  $x_B$  and  $y_B$  are calculated, the location of the centre of buoyancy can be found using the Equation 15.

The code written for centre of buoyancy can be found in Appendix B.

## 5.5 Metacentric radius

Metacentre is a theoretical point through which an imaginary line, passing through the centre of buoyancy and centre of gravity, intersects the other imaginary vertical line, which passes through a new centre of buoyancy, which appeared because the body moved, heeled or tipped in the water. As a result, the metacentre always remains directly above the centre of buoyancy, regardless the movement of the structure (Gregersen, 2012).

To ensure the structure is stable, the metacentre should be located above the centre of gravity. The bigger the distance between the centre of gravity and metacentre, the more stable the structure is.

The distance between the centre of buoyancy and the metacentre is called the metacentric radius ( $\overline{BM}$ ). The metacentre (M) and metacentric radius ( $\overline{BM}$ ) can be seen in Figure 10.

To find the transverse metacentric radius the following equation is used:

$$\overline{BM}_T = \frac{I_T}{V_{disp}} \quad (16)$$

Where,  $\overline{BM}_T$  – transverse metacentric radius,  $I_T$  – transverse moment of inertia of the waterplane,  $V_{disp}$  – the volume of the displaced fluid.

To calculate the moment of inertia of the waterplane, the parallel axis theorem is used.  $I_T$  can be found using the following equation:

$$I_T = i_t + \overline{y}^2 * A_{wp} \quad (17)$$

Where,  $i_t$  – the moment of inertia of the object about an axis through its centre of mass,  $\overline{y}^2$  – the perpendicular distance between rotation axis and object's centre of mass,  $A_{wp}$  – waterplane area.

$i_t$  for the circular shape is calculated using the following formula:

$$i_T = \frac{r^4}{4} \quad (18)$$

Where,  $r$  – is the radius of the circle.

And for the rectangular shape

$$i_T = \frac{bh^3}{12} \quad (19)$$

Where,  $b$  – is the length of the object,  $h$  – is the height of the object.

From the plan and side views of the platform, which can be seen in Figure 14, it is known that there are two different waterplane areas: circle and rectangular. Therefore, the following formulas in Table 5 will be used for the calculations of waterplane area for different structural members.

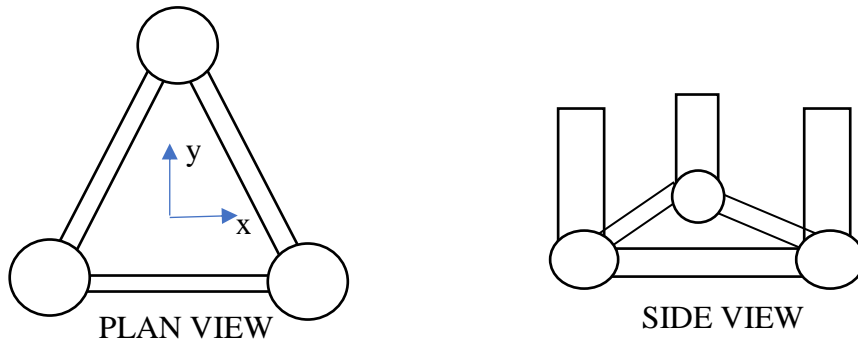


Figure 14 Waterplane areas from plan and side views

Structural member	Waterplane area on longitudinal axis X	Waterplane area on transverse axis Y
Pontoon	$l_p * (2 * r_{pout})$	$\frac{\pi * (2 * r_{pout})^2}{4}$
Column	$\frac{\pi * (2 * r_{ccout})^2}{4}$	$Draft * (2 * r_{ccout})$

Table 5 The formulas, which are used to find the waterplane areas.

The perpendicular distance between the rotation axis, which is located at the centre of gravity and object's centre of mass for each of the submerged structural members, can be seen in the Table 6.

Structural member	Distance $\bar{y}$ on longitudinal axis X	Distance $\bar{y}$ on transverse axis Y
<b>Pontoon no.1</b>	If x coordinate of the centre of gravity is equal to the distance $\frac{l_p}{2}$ , then $\bar{y} = \frac{l_p}{4}$ , otherwise $\bar{y} = \left[ \frac{l_p}{4} - x \right]$	If y coordinate of the centre of gravity is equal to 0, then $\bar{y} = \frac{\sqrt{3} * l_p}{4}$ , otherwise $\bar{y} = \left[ \frac{\sqrt{3} * l_p}{4} - y \right]$
<b>Pontoon no.2</b>	Same as Pontoon no.1	Same as Pontoon no.1
<b>Pontoon no.3</b>	0, because it is on the rotation axis.	Centre of gravity y coordinate
<b>Column no.1</b>	If x coordinate of the centre of gravity is equal to distance $\frac{l_p}{2}$ , then $\bar{y} = 0$ , otherwise $\bar{y} = \left[ \frac{l_p}{2} - x \right]$	If y coordinate of the centre of gravity is equal to distance $\frac{\sqrt{3} * l_p}{2}$ , then $\bar{y} = 0$ , otherwise $\bar{y} = \left[ \frac{\sqrt{3} * l_p}{2} - y \right]$
<b>Column no.2</b>	$[l_p - x]$	Centre of gravity y coordinate
<b>Column no.3</b>	Centre of gravity x coordinate	Centre of gravity y coordinate

Table 6 Distance  $\bar{y}$  on different axis

Now as all the values are known, the transverse and longitudinal metacentric radius can be found. The formula for the longitudinal metacentric radius is the same as for the transverse one, Equation 16. Just the values are taken from the longitudinal axis column instead of transverse.

The code written to find the longitudinal and transverse metacentric radius can be seen in Appendix B

## 5.6 Metacentric height

The metacentric height is the distance between the centre of gravity and metacentre. There are two types of metacentric height: transverse and longitudinal. The metacentric height should always be positive as this is the minimum stability requirement (Aubault, 2016). The negative metacentric height would result in having a negative righting moment. Therefore, the righting moment would act in the same direction as the heeling moment and would make the structure roll over (Gallala, 2013).

The metacentric height can be calculated by using the following formula:

$$\overline{GM} = \overline{KB} + \overline{BM} - \overline{KG} = \overline{KM} - \overline{KG} \quad (20)$$

Where,  $\overline{KB}$  - centroid of underwater volume,  $\overline{BM}$  - metacentric radius,  $\overline{KG}$  - vertical component of the centre of gravity (Aubault, 2016).

As  $\overline{KB}$ ,  $\overline{BM}$  and  $\overline{KG}$  are already found using the previous codes,  $\overline{GM}$  can be found as well. The code for it can be seen in Appendix B

## 5.7 Righting arm

The horizontal distance between the lines of buoyancy and gravity is also known as the righting arm (GZ). The righting arm appears once the structure leans. To make sure the structure is stable the righting arm should always be positive (Aubault, 2016).

The formula used to calculate the righting arm for the small angles of heel, less than 7° or 10° can be seen below:

$$\overline{GZ} = \overline{GM} * \sin \phi \quad (21)$$

Where,  $\overline{GM}$ - metacentric height,  $\phi$  - angle of heel.

Usually righting arm is illustrated on graph where x-axis is the heeling angle, varying from 0° to 90° in 10° increments, and the y-axis is the righting arm (Gillmer, 1982). This method helps to visualise how the righting arm varies depending of what size is the heeling angle.

If the righting arm is being calculated for the larger angles than 7° or 10°, the following formula can be used:

$$\overline{GZ} = \overline{KN} - \overline{KG} * \sin\phi \quad (22)$$

Where,  $\overline{KN}$ - is the distance from the keel to the vertical line of action of buoyancy, which varies depending on the heeling angle and the displacement,  $\overline{KN}$  can be seen in the Figure 15,  $\overline{KG}$  - is the centre of gravity.

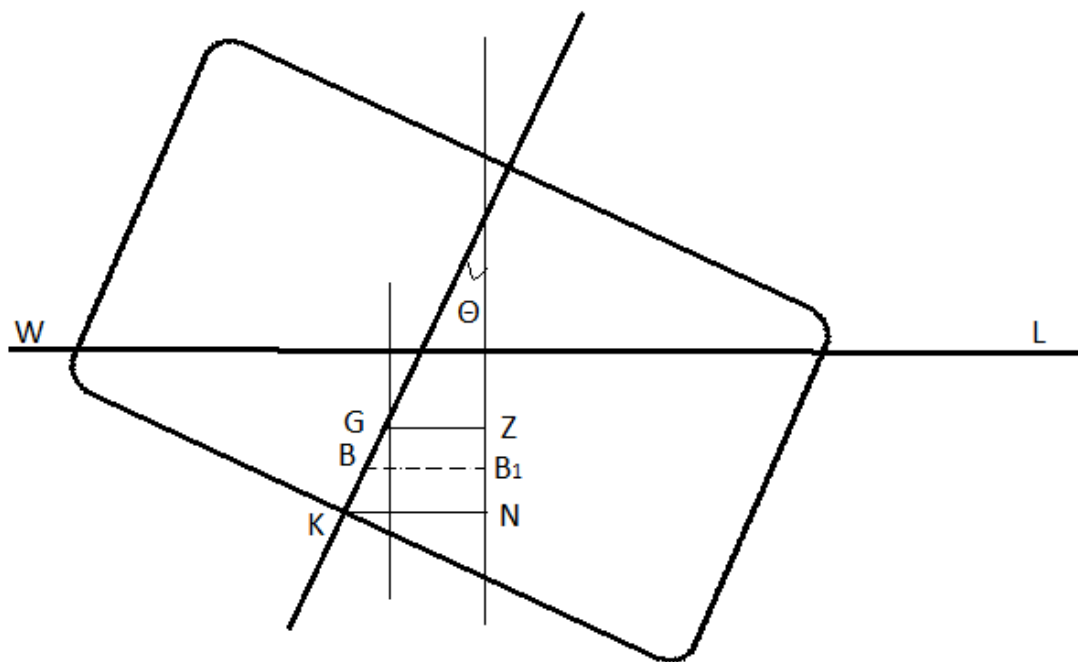


Figure 15 Structure measurements when it heels

This time to produce the values for the righting arm the Equation 21 has been used. The code written for the righting arm can be seen in Appendix B.

# CHAPTER SIX – PROGRAMMING

## 6.1 Input

To write the codes for the computations, the programming language Fortran has been used.

First of all, flowcharts were prepared to show the sequence of the process. An example of the flowchart used to find the centre of buoyancy can be seen below in Figure 16.

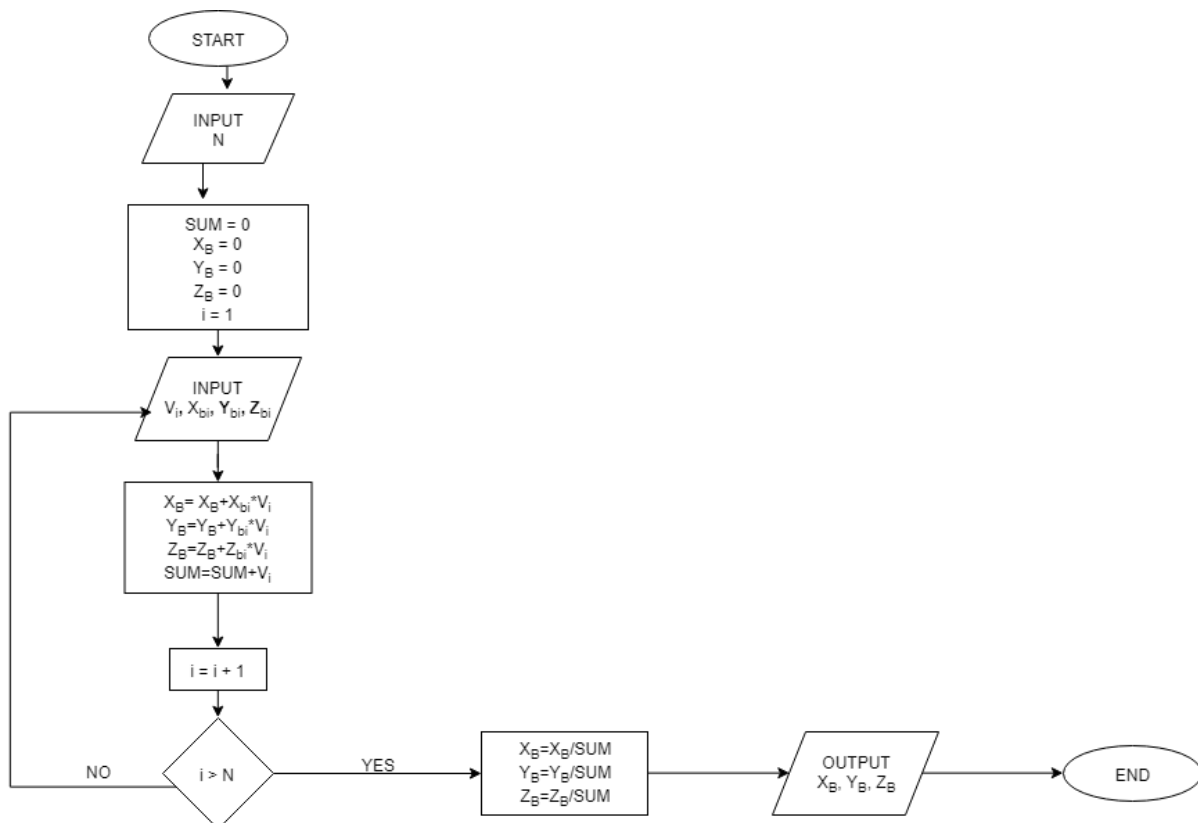


Figure 16 Centre of buoyancy flowchart

As it can be seen from the flowchart, the first step is to have an input data, which will be used to run the calculations. Therefore, the files INPUT.txt together with INPUT\_INSTRUCTIONS.txt have been created. The user who wants to use the program and run the computations will first need to open the file called INPUT\_INSTRUCTIONS.txt and following the instructions given in that file write down the values of his structure in the file INPUT.txt. How both of these files look like can be seen in Appendix A.

For the Carlos Wong platform, the values inputted in INPUT.txt file were the same as the ones in Table 2.

# CHAPTER SEVEN – RESULTS

## 7.1 Results

It can be seen that the codes from Appendix B take the values for the calculations from the input file INPUT.txt. The results achieved after the codes run can be seen in the Table 7. This table shows the location of centre of gravity if the additional weight of ballast is added to consideration.

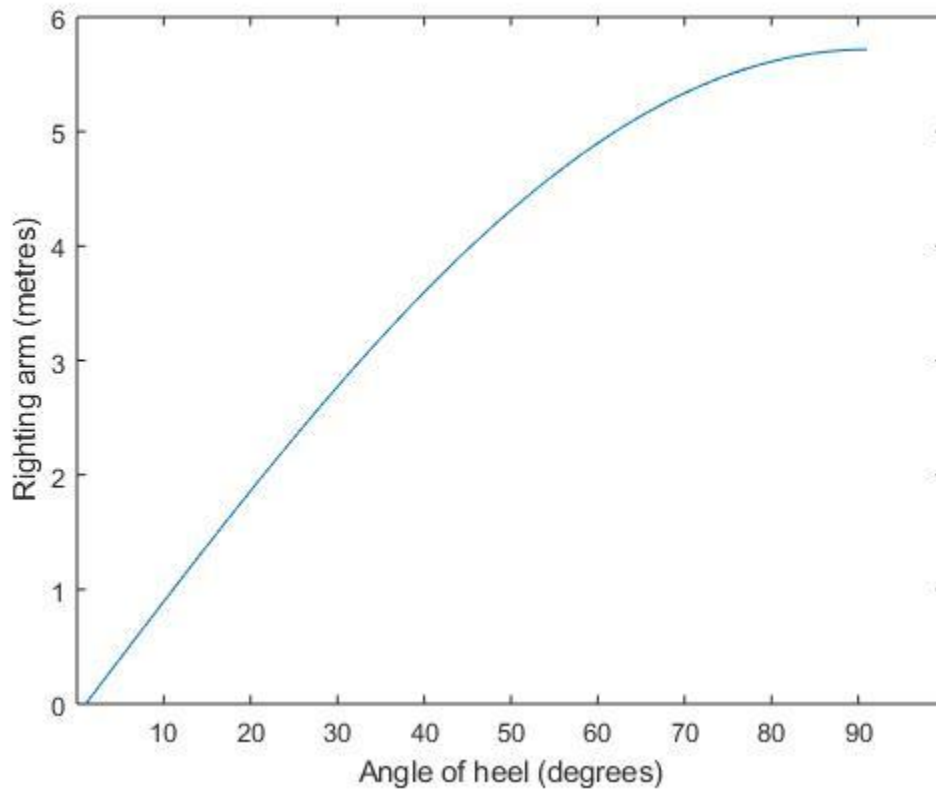
	<b>Result</b>
Weight of the columns	$4.58 \cdot 10^7$ kg
Weight of the turbines	$2.05 \cdot 10^7$ kg
Weight of the pontoons	$1.57 \cdot 10^8$ kg
Weight of the ballast	$2.33 \cdot 10^8$ kg
Weight of the whole structure	$4.56 \cdot 10^8$ kg
$V_{disp}$	45382.5 m <sup>3</sup>
Draft	12.12 m
Centre of gravity (z, x, y)	11.03, 132.28, 77.91
Centre of Buoyancy (z, x, y)	4.25, 132.29, 77.95
Metacentric radius $BM_T, BM_L$	1.46, 2.57
Righting moment	5.72

Table 7 Achieved results

After all the required values are found, the curve of the static stability can be drawn. This curve is a plot between the righting arm and the angle of heel. It relates the metacentric height to the angle of heel. The structure's stability can be judged directly by just looking at this curve. This curve shows the highest angle the structure can heel before it capsizes. Also, it helps to predict how big can be the force from the wind, waves etc. until the structure no longer can absorb it and the stability will be affected. (Chakraborty, n.d.).

To draw such a graph, programming language MATLAB will be used. Firstly, using the code from Fortran (seen in Appendix B), the values of different righting arms for different heeling angles are found. These values are then saved to the file called Data.txt. This file with the achieved values can be seen in Appendix E. Then using these values and the code written in MATLAB, which can be found in Appendix D, the curve of static stability was plotted for the

heeling angle varying from  $0^\circ$  to  $90^\circ$ . This can be seen in Figure 17.



*Figure 17 Curve of static stability with a heeling angle varying from 0 to 90 degrees.*

However, from the curve with the heeling angle varying from  $0^\circ$  to  $90^\circ$  it cannot be seen exactly which point of the curve is the highest point. Therefore, another curve with heeling angle varying from  $0^\circ$  to  $180^\circ$  was made. This curve can be seen in Figure 18.

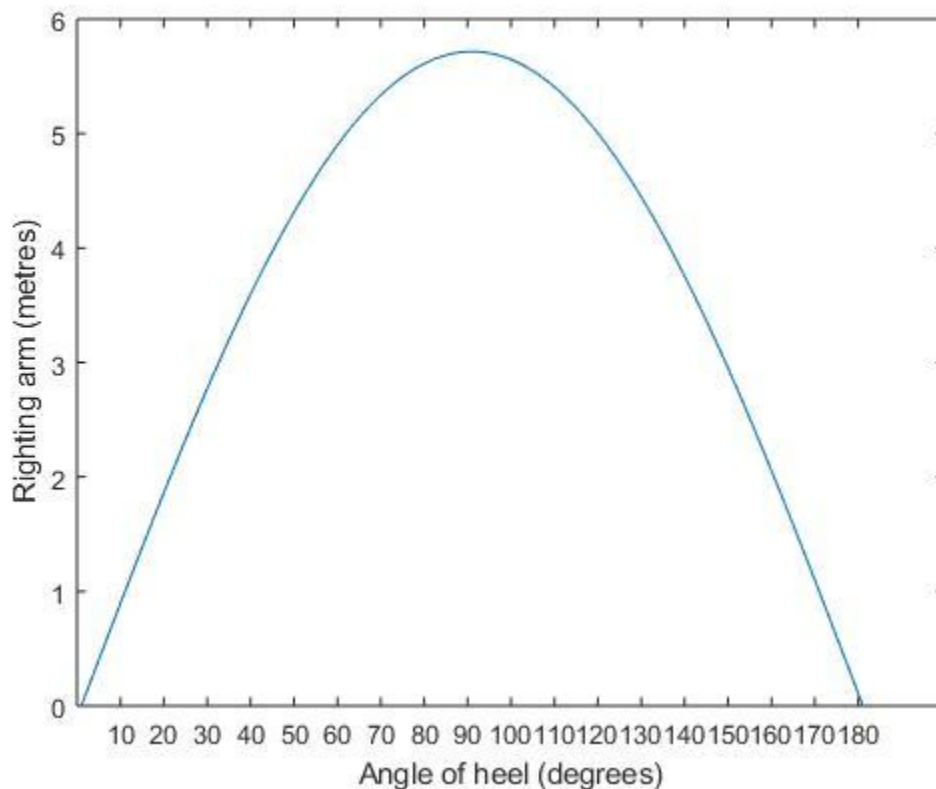


Figure 18 Curve of static stability with heeling angle varying from 0 to 180 degrees

From this graph, it can be seen that the heeling angle at which a maximum righting arm happens, is  $90^\circ$ . This means that the structure at this angle uses the most energy to put it back to its initial position. The value of maximum righting arm appeared to be 5.72 m. Also, if the righting arm is multiplied by the displacement, the value of the maximum heeling moment, that the structure can sustain before rolling over, can be found.

What is more, from the area under the static stability curve, the amount of energy that the structure can absorb from the external forces such as wind, waves etc. can be told.

However, maximum heeling angle of  $90^\circ$  seems like a too large of a value as, at this position, one side of the structure would be already submerged into the water. Therefore, I believe the curve of static stability is not right and maybe instead of using the Equation 21 to find the righting arm for small angles, the Equation 22 should have been used.

However, due to the time limit, I could not find the values of  $\overline{KN}$ , which requires the value of the trim and the new draft for when the structure is heeling to be found. And therefore, the correct curves of static stability could not be produced, or the correct maximum heeling angle could not be found.

Although, if that would not be the case and the stability of the structure would need to be improved, it could be done by changing the location of the centre of gravity. For example, if the centre of gravity in vertical direction would go downwards, structure's righting arm would increase and, therefore, the structure would become more stable than before.

## CHAPTER EIGHT – CONCLUSION

This thesis explained why it is important to generate energy from the renewable sources. Different types of renewable energy sources were mentioned, and offshore wind turbines were compared with the onshore ones. The stability requirements for the offshore wind turbine were stated, and it was explained how to achieve some of the required values in order to ensure the stability of the offshore wind turbine.

It was decided to use Carlos Wong semi-submersible triangular raft with three turbines to proceed with the hydrostatic analysis. The values of achieved results such as draft, centre of gravity etc. were showed and explained. To achieve these results and run the calculations, help of programming languages Fortran and MATLAB was used. The codes used for these calculations will be able to be reused in the future by other users. The instruction file, together with the input file, were created and provided for them to do the stability analysis of their own structure.

However, the created curve of static stability seems to be wrong as it gives a very high maximum heeling angle. This was not fixed due to the difficulties faced during the initial stages of planning the project. These difficulties consist of: losing time when trying to learn how to code or to understand the naval architecture principles. As well as, getting wrong results from my calculations as the weight of the ballast was not considered in the beginning. Due to this, there was no time to provide a damage stability analysis.

In the future, to prepare the full buoyancy and stability analysis during different conditions, the values such as  $\overline{KN}$ , trim and others should be calculated as well.

## REFERENCES

- Adepipe, O., Abolarin, M. and Mamman, R. (2018). A Review of Onshore and Offshore Wind Energy Potential in Nigeria. In: *Materials Science and Engineering*. p.4.
- Aubault, A. and Ertekin, R. (2016). Stability of Offshore Systems. In: M. Dhanak and N. Xiros, ed., *Springer Handbook of Ocean Engineerin*. Springer, Cham, p.774.
- Aubault, A. and Ertekin, R. (2016). Stability of Offshore Systems. In: M. Dhanak and N. Xiros, ed., *Springer Handbook of Ocean Engineerin*. Springer, Cham, p.764.
- Aubault, A. and Ertekin, R. (2016). Stability of Offshore Systems. In: M. Dhanak and N. Xiros, ed., *Springer Handbook of Ocean Engineerin*. Springer, Cham, p.775.
- Chakraborty, S. (n.d.). Ship Stability – Understanding Curves of Static Stability. [Blog].
- Department for Business, Energy & Industrial Strategy (2018). *UK Energy Statitics, Q1 2018*.
- Energy and Climate Intelligence Unit (2018). *Net zero: power*.
- Energy4me.org. (2018). *Energy Source Comparison | energy4me*. [online] Available at: <http://energy4me.org/all-about-energy/what-is-energy/energy-sources/>
- Equinor (n.d.). *HYWIND illustration*. [image] Available at: <https://www.equinor.com/en/news/hywindscotland.html> [Accessed 20 Mar. 2019].
- Equinor (n.d.). *Hywind line-up Scott Monument Edinburgh*. [image] Available at: <https://www.equinor.com/en/news/hywindscotland.html> [Accessed 20 Mar. 2019].
- Esteban, M., Diez, J., López, J. and Negro, V. (2011). Why offshore wind energy? *Renewable Energy*, 36(2), pp.444-450.
- Esteban, M., Diez, J., López, J. and Negro, V. (2011). *Distribution of the offshore wind megawatts in operation in the different countries at the beginning of the year 2009*. [image].
- Esteban, M., Diez, J., López, J. and Negro, V. (2011). *Growth of the offshore wind energy capacity since 1990 to 2007*. [image].
- Esteban, M., Diez, J., López, J. and Negro, V. (2011). *Lifetime emissions of carbon dioxide for various power generation technologies*. [image].

- Gallala, J. (2013). *Hull Dimensions of a Semi-Submersible Rig. A Parametric Optimization Approach*. Norwegian University of Science and Technology.
- Gillmer, T. and Johnson, B. ed., (1982). GENERAL STABILITY AT LARGE ANGLES OF HEEL. In: *Introduction to Naval Architecture*. p.148.
- Gregersen, E. and Singh, A. (2012). Metacentre. In: *Encyclopedia Britannica*.
- Herzog, A., Lipman, T., Edwards, J. and Kammen, D. (2001). Renewable Energy: A Viable Choice. *Environment: Science and Policy for Sustainable Development*, 43(10), pp.8-20.
- Statoil (2015). *Hywind Scotland Pilot Park*. Environmental Statement. p.21.
- Iglesia, G., Albuquerque, P., Agüero, J., Tufiño, G., Andrea, S. and Tufiño, M. (2017). *Evaluating different types of renewable energy for implementation in schools*. Mexico.
- International Atomic Energy Agency (2001). *Present and future environmental impact of the Chernobyl accident*. Vienna: IAEA.
- Lamei, A. (2018). *Drawings of the Triangular Platform with the Turbines: Front View*.
- Lamei, A. (2018). *Drawings of the Triangular Platform with the Turbines: Isometric View*.
- Li, B., Liu, K., Yan, G. and Ou, J. (2011). Hydrodynamic comparison of a semi-submersible, TLP, and Spar: Numerical study in the South China Sea environment. *Marine Science and Application*, 10, pp.306-314.
- Lotha, G. (2018). *Centre of gravity / physics*.
- McCall, C. (2016). Chernobyl disaster 30 years on: lessons not learned. *The Lancet*, 387(10029), pp.1707-1708.
- Morse, E. (2013). non-renewable energy. In: *National Geographic Society*.
- Parsons, J. (n.d.). Center of Buoyancy: Definition & Formula. In: *Introduction to Engineering*
- Sen, Z. (2008). *Solar Energy Fundamentals and Modeling Techniques*. Springer-Verlag London Limited, pp.3-4.
- Sen, Z. (2008). *Solar Energy Fundamentals and Modeling Techniques*. Springer-Verlag London Limited, p.10.
- Spon, E., Byrne, O., Spon, E. and Spon, F. (1874). *pons' dictionary of engineering, civil, mechanical, military, and Naval, Volume 2*. p.1205.

Statoil (2015). *Hywind Scotland Pilot Park*. Environmental Statement Non Technical Summary. p.7.

Surface Officer Warfare School (n.d.). *Principles of Stability*. Damage Control Training.

Wong, C. (2015). Wind tracing rotational semi-submerged raft for multi-turbine wind power generation. In: *EWEA Offshore*

Wong, C. (2015). *Three turbines triangular raft*. [image].

World Energy Council (2016). *World Energy Resources / 2016*. World Energy Council 2016, p.2.

World Energy Council (2016). *World Energy Resources / 2016*. World Energy Council 2016, p.4.

World Energy Council (2016). *COMPARATIVE PRIMARY ENERGY CONSUMPTION OVER THE PAST 15 YEARS*. [image] Available at: <https://www.worldenergy.org/wp-content/uploads/2016/10/World-Energy-Resources-Full-report-2016.10.03.pdf> [Accessed 20 Mar. 2019].

# APPENDICES

## Appendix A – Input and Instruction files

Instructions.txt - Notepad

File Edit Format View Help

To run the program, please follow the instructions and input the following values in their assigned line in the INPUT.txt file and press SAVE.

line 1 - density of the water in kg/m<sup>3</sup>  
line 2 - density of the material used in kg/m<sup>3</sup>  
line 3 - length of the pontoon in metres  
line 4 - outer radius of the pontoon in metres  
line 5 - inner radius of the pontoon in metres  
line 6 - outer radius of the column in metres  
line 7 - inner radius of the column in metres  
line 8 - height of the column in metres  
line 9 - mass of the turbine kg  
line 10 - outer radius of the turbine's tower in metres  
line 11 - height of the tower in metres  
line 12 - create an empty line

INPUT.txt - Notepad

File Edit Format View Help

**1025**  
**2400**  
**264**  
**4**  
**3.65**  
**7**  
**6.6**  
**38**  
**697000**  
**3**  
**177.6**

## Appendix B – Hydrostatic analysis code

```

program righting_arm
real ::
lp,qw,qc,ht,g,pi,wt,rp2,wp,d,mt,rpout,rpin,rcc2,rccout,rccin,hcc,W,z1,z2,z3,KGz,x11,x12,x13,x21,x22,x23
,x31,x32,rtout,rt2
real:: kgp,kgcc,kgc,A1,A2,A,Zb,Xb,Yb,three,KBz,KBx,KBy
real:: Zb1,Zb2,Dc2,Dp2,Vp,Vc,Xb11,Xb12,Xb13,Xb21,Xb22,Xb23,Yb11,Yb12,Yb13,Yb21,Yb22,Yb23
real :: x33,KGx,KGy,y11,y12,y13,y21,y22,y23,y31,y32,y33,KM,GM,GZ,i,wb
real:: IT1,IT2,IT3,IT4,IT5,IT6,rccout4, rpout4,
IL1,IL2,IL3,IL4,IL5,IL6,Y1,Dp,Dp3,Y2,Y3,BMT,Y5,d3,Y6,Y7,BML
!d- draft
!rpout,rpin- outer and inner radius of pontoons
!rtout,rtin- outer and inner radius of the tower
!rccout,rccin - outer and inner radius of the column
!! cc-column
!t-tower
!p-pontoons
!rt2,rp2,rcc2- these values are squared
!z-distance from the keel to the objects centre of mass in z (vertical direction)
!Y1-distance from parallel axis
!wb-weight of ballast,70%

open(1, file = 'INPUT.txt', status = 'old')

read(1, *) qw
read(1, *) qc
read(1, *) lp
read(1, *) rpout
read(1, *) rpin
read(1, *) rccout
read(1, *) rccin
read(1, *) hcc
read(1, *) mt
read(1, *) rtout
read(1, *) ht

close(1)

g=9.8
pi=3.14

rp2=(rpout*rpout)-(rpin*rpin)
rcc2=(rccout*rccout)-(rccin*rccin)

wb=((pi*rpin*rpin)*lp*qw*g)*0.7
wp=((pi*rp2)*lp*qc*g)
wcc=(pi*rcc2*hcc*qc*g)
wt=(mt*g)

W=(wt+wp+wcc+wb)*3

Vdisp=W/(qw*g)

d=(Vdisp-((pi*rpout*rpout*lp)*3))/((pi*rccout*rccout)*3)

print*,"draft is",d

wb=wb*3
wp=wp*3
wt=wt*3
wcc=wcc*3

wp=wp+wb

!centre of gravity
!z direction:
z1=rpout
z2=(hcc/2)
z3=hcc+(ht/2)

```

```

KGz=(((wp*z1)+(wcc*z2)+(wt*z3))*3)/W)/3

!x direction:
!1st turbine , closest to coordinate system
x11=lp/2
x21=rccout
x31=rtout
!2nd turbine
x12=lp/4
x22=lp/2
x32=lp/2
!3rd turbine
x13=(lp/2)+(lp/4)
x23=lp
x33=lp

KGx=(((wp*(x11+x12+x13)))+(wcc*(x21+x22+x23)))+(wt*(x31+x32+x33)))/W)/3

!ydirection
!1st turbine
y11=rpout
y21=rccout
y31=rtout
!2nd turbine
three=3
y12=((sqrt(three))*lp)/4
y22=((sqrt(three))*lp)/2
y32=((sqrt(three))*lp)/2
!3rd turbine
y13=((sqrt(three))*lp)/4
y23=rccout
y33=rtout

KGy=(((wp*(y11+y12+y13)))+(wcc*(y21+y22+y23)))+(wt*(y31+y32+y33)))/W)/3

print*, "Centre of Gravity coordinates are z,x,y", KGz,KGx,KGy

!Centre of Buoyancy
!z direction
Dp2=(rpout*2)*(rpout*2)
Dc2=(rccout*2)*(rccout*2)
Zb1=3*Dp2*lp*rpout
Zb2=3*Dc2*d*(d/2)
Zb=(pi/(4*Vdisp))*(Zb1+Zb2)

!x-direction
!Volumes
Vp=Dp2*lp
Vc=Dc2*d

!for pontoons:
Xb11=lp/2
Xb12=lp/4
Xb13=(3*lp)/4

!for submerged columns:
Xb21=rccout
Xb22=lp/2
Xb23=lp

Xb=(pi/(4*Vdisp))*((Vp*(Xb11+Xb12+Xb13)))+(Vc*(Xb21+Xb22+Xb23))

!ydirection:
!for pontoons:
Yb11=rpout
Yb12=sqrt(3*lp*lp)/4
Yb13=sqrt(3*lp*lp)/4

!for submerged columns:
Yb21=rccout
Yb22=sqrt(3*lp*lp)/2
Yb23=rccout

```

```

Yb=(pi/(4*Vdisp))*((Vp*(Yb11+Yb12+Yb13))+Vc*(Yb21+Yb22+Yb23))

print*, "Centre of Buoyancy coordinates are z,x,y", Zb,Xb,Yb

!Transverse metacentric radius

!column no.1
rccout4=rccout*rccout*rccout*rccout

if (KGx == lp/2) then
    Y1 = 0
else
    Y1 =ABS((lp/2)-KGx)
end if

IT1=((pi*rccout4)/4)+(Y1*(pi*rccout*rccout))

!column no.2
IT2=((pi*rccout4)/4)+(ABS(lp-KGx))*(pi*rccout*rccout))

!column no.3
IT3=((pi*rccout4)/4)+(ABS(KGx))*(pi*rccout*rccout))

!pontoon no.1
Dp=rpout/2
Dp3=Dp*Dp*Dp

if (KGx == lp/2) then
    Y2 = lp/4
else
    Y2 =ABS((lp/4)-KGx)
end if

IT4=((lp*Dp3)/12)+Y2*(lp*Dp)

!pontoon no.2

if (KGx == lp/2) then
    Y3 = lp/4
else
    Y3 =ABS((lp/4)-KGx)
end if

IT5=((lp*Dp3)/12)+Y3*(lp*Dp)

!pontoon no.3

IT6=((lp*Dp3)/12)
!Y4=0 because it is on the axis

BMT= (IT1+IT2+IT3+IT4+IT5+IT6)/Vdisp

!longitudinal metacentric radius

!column no.1

d3=d*d*d

if (KGy ==sqrt(3*lp*lp)/2) then
    Y5 = 0
else
    Y5 =ABS((sqrt(3*lp*lp)/2)-KGy)
end if

IL1=((rccout*2)*d3)/12)+Y5*(d*rccout*2)

!column no.2

IL2=((rccout*2)*d3)/12)+ABS(KGy)*(d*rccout*2)

```

```

!column no.3
IL3=((rccout*2)*d3)/12+ABS(KGy)*(d*rccout*2)

!pontoon no.1
rpout4=rpout*rpout*rpout*rpout

if (KGy ==0) then
    Y6 = sqrt(3*lp*lp)/4
else
    Y6 =ABS((sqrt(3*lp*lp)/4)-KGy)
end if

IL4=((pi*rpout4)/4)+Y6*(pi*rpout*rpout)
!pontoon no.2

if (KGy ==0) then
    Y7 = sqrt(3*lp*lp)/4
else
    Y7 =ABS((sqrt(3*lp*lp)/4)-KGy)
end if

IL5=((pi*rpout4)/4)+Y7*(pi*rpout*rpout)

!pontoon no.3

IL6=((pi*rpout4)/4)+ABS(KGy)*(pi*rpout*rpout)

BML=(IL1+IL2+IL3+IL4+IL5+IL6)/Vdisp

print*, "Transverse metacentric radius, with respect to Centre of Gravity, is", BMT
print*, "Longitudinal metacentric radius,with respect to Centre of Gravity, is", BML

!KM
KM=Zb+(BMT+KGz)

!GM
GM=KM-KGz
print*, "righting moment is", KM

open(2, file='data.dat', status = 'old')
do i=0, 90
    GZ=GM*sin( i * pi / 180 )
    write(2, *) GZ
end do
close(2)

end program righting_arm

```

## Appendix C – Achieved results

C:\WINDOWS\SYSTEM32\cmd.exe

```
Vdisp 45382.5
draft is 12.1158
wp,wcc,wt,wb 3.895747E+08 4.580058E+07 2.049180E+07 2.329639E+08
Wtotal 4.558670E+08
Centre of Gravity coordinates are z,x,y 11.0271 132.279 77.9084
Centre of Buoyancy coordinates are z,x,y 4.25359 132.288 77.9543
Transverse metacentric radius, with respect to Centre of Gravity, is 1.46302
Longitudinal metacentric radius, with respect to Centre of Gravity, is 2.57446
righting moment is 5.71661
C:\Users\Ieva\Desktop\fortran>
```

## Appendix D – MATLAB code

- a) Heeling angle varies from 0 to 90 degrees.

```
function y = righting_arm_graph()
    data = fopen('data90.dat', 'r');
    data2 = fscanf(data, '%f');
    figure
    plot(data2)
    xlabel('Angle of heel (degrees)'), ylabel('Righting arm (metres)')
    xticks(10:10:90)
end
```

- b) Heeling angle varies from 0 to 180 degrees.

```
function y = righting_arm_graph()
    data = fopen('data180.dat', 'r');
    data2 = fscanf(data, '%f');
    plot(data2)
    xlabel('Angle of heel (degrees)'), ylabel('Righting arm (metres)')
    xticks(10:10:180)
end
```

Appendix E – data.txt file, righting arm values (highlighted value-  
maximum righting arm)

0.000000	1.95424	3.67301	4.94921	5.62906
9.971800E-02	2.04766	3.74887	4.99836	5.64559
0.199406	2.14045	3.82358	5.04599	5.66040
0.299033	2.23259	3.89713	5.09209	5.67348
0.398569	2.32404	3.96949	5.13663	5.68485
0.497983	2.41480	4.04064	5.17962	5.69448
0.597246	2.50481	4.11057	5.22102	5.70238
0.696328	2.59407	4.17924	5.26084	5.70854
0.795197	2.68253	4.24664	5.29906	5.71297
0.893825	2.77018	4.31275	5.33566	5.71566
0.992181	2.85699	4.37755	5.37064	5.71661
1.09023	2.94293	4.44102	5.40399	5.71582
1.18796	3.02797	4.50313	5.43569	5.71329
1.28532	3.11209	4.56387	5.46574	5.70902
1.38229	3.19526	4.62323	5.49412	5.70301
1.47883	3.27746	4.68118	5.52084	5.69527
1.57493	3.35866	4.73770	5.54587	5.68580
1.67055	3.43885	4.79278	5.56921	5.67459
1.76566	3.51798	4.84640	5.59087	5.66166
1.86024	3.59605	4.89855	5.61081	5.64701

---

5.63064	4.95376	3.67999	1.96280	9.103973E-03
5.61255	4.90324	3.60312	1.86884	
5.59276	4.85123	3.52515	1.77432	
5.57126	4.79774	3.44611	1.67926	
5.54807	4.74279	3.36603	1.58368	
5.52319	4.68639	3.28492	1.48763	
5.49663	4.62858	3.20281	1.39112	
5.46840	4.56935	3.11972	1.29419	
5.43850	4.50873	3.03569	1.19686	
5.40695	4.44674	2.95073	1.09917	
5.37375	4.38340	2.86487	1.00115	
5.33892	4.31872	2.77814	0.902816	
5.30247	4.25273	2.69057	0.804211	
5.26440	4.18545	2.60218	0.705363	
5.22472	4.11689	2.51299	0.606299	
5.18346	4.04708	2.42305	0.507053	
5.14062	3.97604	2.33236	0.407650	
5.09622	3.90378	2.24096	0.308124	
5.05026	3.83034	2.14889	0.208503	
5.00277	3.75573	2.05616	0.108821	